

Land subsidence prediction over an off-shore reservoir in Italy by a sequential data-integration approach

L. Gazzola¹, M. Ferronato¹, P. Teatini¹, C. Zoccarato¹

¹ Department of Civil, Environmental and Architectural Engineering, University of Padova, Padova, Italy

laura.gazzola.1@phd.unipd.it

Session: Modelling and Matching – Strategies & Pathways

Keywords: Data Assimilation; Subsidence Modelling; Uncertainty Quantification

Introduction

Uncertainty in prediction of land subsidence due to hydrocarbon extraction from productive reservoirs can be reduced by exploiting the available measurements. A comprehensive workflow (Gazzola et al., 2021) combining different Data Assimilation (DA) approaches has been developed, with the aim to account for and reduce uncertainties by progressively training a numerical model as new data are integrated. After identifying the most influential uncertain factors and their confidence intervals, a forward geomechanical model provides the initial forecast ensembles of Monte Carlo realizations. A preliminary diagnosis of the forecast ensembles is carried out by the χ^2 -test (Fokker et al., 2016) and the Red Flag (RF) technique (Nepveu et al., 2010), in order to evaluate the actual representativeness of the monitored process, e.g., land settlements recorded by a GNSS station or deep compaction from radioactive markers. Then, if the preliminary diagnostic response is positive, DA is used to constrain the ensembles with the available measurements, otherwise new ensembles should be built. In the present work, the model is updated through the Ensemble Smoother (ES) technique (Leeuwen & Evensen, 1996), which is an ensemble-based non-sequential algorithm that provides a simultaneous update of both the state and parameter ensembles by combining prior information, measurements, and the solution of the numerical model. The ES outcome is the most reliable prediction according to the currently available observations. The updated parameters from ES are used as new input for the geomechanical model to create new forecast ensembles. The latter are integrated in the workflow when new measurements become available and so the overall procedure can be repeated starting from the diagnostic step. The repetition in time during and after the reservoir production life allows for a progressive improvement in the prediction confidence and reliability. For more details, the reader is referred to Gazzola et al. (2021).

This work presents an application of the proposed approach to a real-world off-shore hydrocarbon reservoir buried in the Adriatic basin, Italy.

Real-world application on an off-shore hydrocarbon reservoir

The area of interest is located off-shore in the Adriatic Sea about 60 km from the Italian coastline. The reservoir structure is an anticline with two culminations within a turbiditic Pleistocene formation, resulting in a complex multi-pay system with more than one hundred active layers of meter- to centimeter-thickness lying between 900 and 1800 m below mean sea level. Pressure data, different from layer to layer, are measured for 13 years (today) and predicted over the following 42 years by a

history-matched reservoir model (Fig. 1a). In this work, we assume the pressure behaviour in time and space to be deterministic, with the main uncertainties related to the nature and value of the geomechanical parameters governing the reservoir rock behaviour. We consider two constitutive laws for the active layers: a standard modified Cam Clay (MCC) and a visco-elasto-plastic (VEP) model (Isotton et al., 2019). Uncertainties are associated with the most influential parameters for these laws: the modified compression index λ^* for MCC, and λ^* and the initial overconsolidation ratio R for VEP. The range of variability of these parameters is estimated from laboratory tests and used to generate two initial forecast ensembles (Tab. 1). Different kinds of measurements in different time periods become available during the reservoir lifetime (Fig. 1b). In particular, two GNSS stations record the sea bottom displacements over time from year 4, a spatially distributed measure of the seabed movements is given by two bathymetric surveys at years 3 and 10, and deep compaction data are collected by radioactive markers from year 6.

LAW	UNCERTAIN PARAMETER DISTRIBUTION
MCC	$\ln(\lambda^*) \sim \mathcal{N}(-2.58; 0.44)$
VEP	$\ln(\lambda^*) \sim \mathcal{N}(-2.58; 0.44)$ $R \sim U(1.1; 1.5)$

Table 1 Characterization of the forecast ensembles. Constitutive law and prior distribution (with mean and variance) of the parameters λ^* and R .

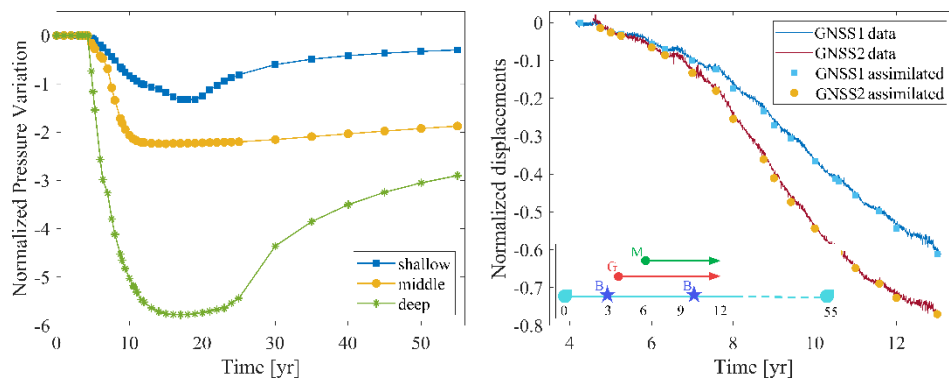


Figure 2 a) Pressure change evolution over time: normalized values in a shallow, middle and deep layer of the reservoir. b) Surface displacements over time measured by the two GNSS stations (dots are the assimilated values). On the bottom left corner the timeline shows the 55 years of pressure data along with the availability of the GNSS data (red arrow), the bathymetric surveys (purple stars) and the radioactive marker measurements (green arrows).

Modelling results

The availability of new measurements dictates the frequency of the subsidence model update. In this case, the model is updated every three years starting from year 7. The number of assimilated measurements at each update is reported in Table 2.

The initial prediction relies on the ensembles created from the estimated parameter ranges (Tab. 1) with both the MCC and the VEP constitutive behaviour. Such ensembles turn out to be very distributed, with surface displacement that can vary by about a factor of 20. At year 7, three years of GNSS measurements allow for a first diagnosis of the ensemble quality. The value of the χ^2 turns out to be equal to 1223 for the MCC and 16 for the VEP ensemble, while RF does not provide significant indications. This points out the better suitability of the VEP model, which presents a lower χ^2 value. However, considering the limited amount of available data, both the ensembles are kept for the update step. The ES application provides a dramatic reduction of the initial uncertainty. Fig. 2 shows the (normalized) land subsidence at a GNSS location in time before (grey) and after (red) the ES, while Fig. 3 reports the Cumulative Distribution Function (CDF) for the uncertain parameters.

YEAR	MEASUREMENTS			
	G	M	B	TOT
7	13	-	-	13
10	25	12	-	37
13	37	20	13	70

Table 2 Amount of available measurements for each assimilation date, respectively recorded from the GNSS stations (G), radioactive markers (M) and the bathymetry (B).

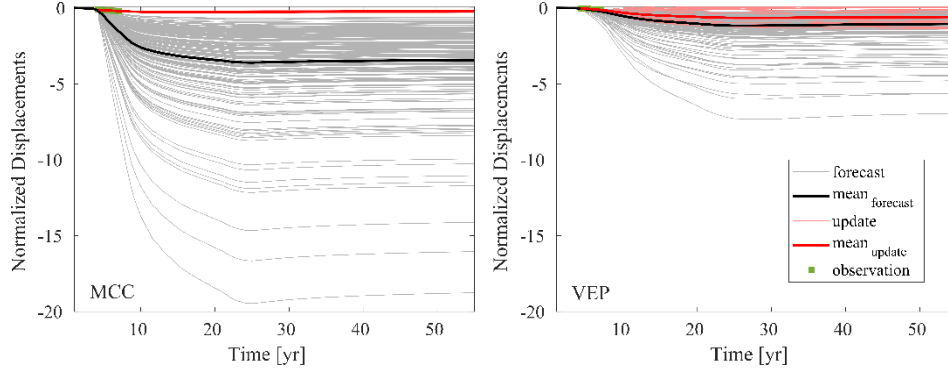


Figure 2 Forecast (grey) and updated (red) displacements in time with ES at year 7.

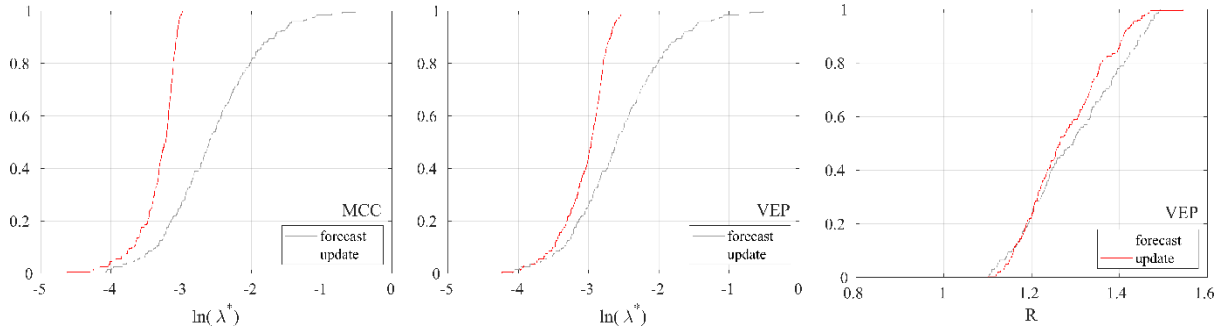


Figure 3 CDF of $\ln(\lambda^*)$ for MCC (left) and VEP (center), and CDF of the parameter R for VEP (right) at year 7.

Both the models are well constrained through the available measurements for both the states and the parameters ensembles. The mean and variance of the updated parameter ensembles are used to create the parameter distributions for the generation of the new forecast ensembles. In particular, the update distribution for the MCC is $\ln(\lambda^*) \sim \mathcal{N}(-3.32; 0.08)$, while for the VEP model the updated distributions are $\ln(\lambda^*) \sim \mathcal{N}(-3.05; 0.11)$ and $R \sim \mathcal{N}(1.28; 0.01)$.

A new model update is carried out at year 10. In addition to the data from the GNSS stations, deep compaction measurements are available at this time. The results of the diagnostic step are consistent with those at year 7, pointing again to the unfitting of the MCC model that is now discarded. The ES application on the new ensemble built on the VEP model is shown in Fig. 4. The newly assimilated measurements allow to further reduce the model uncertainties, in both the states and the parameter prediction. This is particularly true for the displacement update, where the forecast is becoming more and more reliable. On the parameter side, distributions are also less uncertain, but the update is not fully satisfactory, because the update of the parameter R includes some non-physical values ($R < 1$). From those updates, the new parameter ranges are derived: $\ln(\lambda^*) \sim \mathcal{N}(-3.13; 0.05)$ and $R \sim \mathcal{N}(1.08; 0.002)$. In the new ensemble construction, the non-physical values of R , which are located just on the tail of the distribution, are discarded.

At year 13 we carry out the last model update including the data-set from the bathymetric surveys. The diagnostic step confirms the representativeness of the current ensemble. The results of the final model update through the ES application are shown in Fig. 5. If we compare the resulting update ensemble with the initial forecast, a dramatic reduction of the uncertainty can be observed. The numerical model has progressively learned from the observations and its reliability is substantially improving. Notice also that, after the assimilation of the new measurements, the updated parameter distribution of R regains a physical meaning. This model represents the most reliable land subsidence prediction available to date.

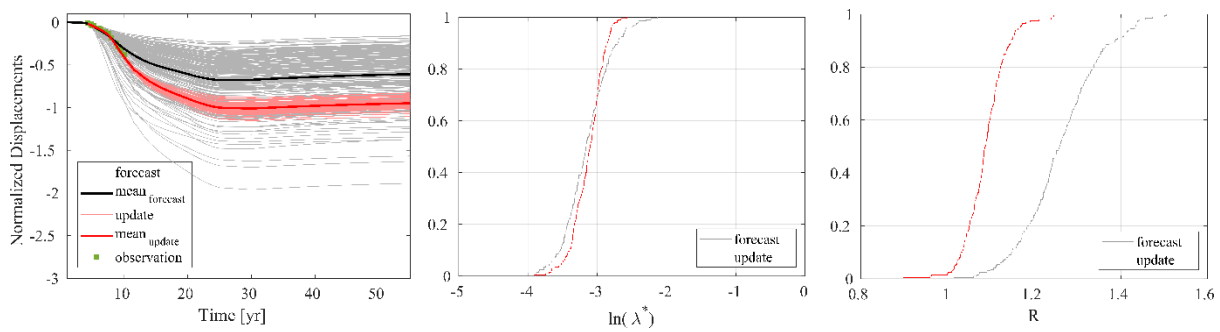


Figure 4 ES application for the VEP model at year 10.

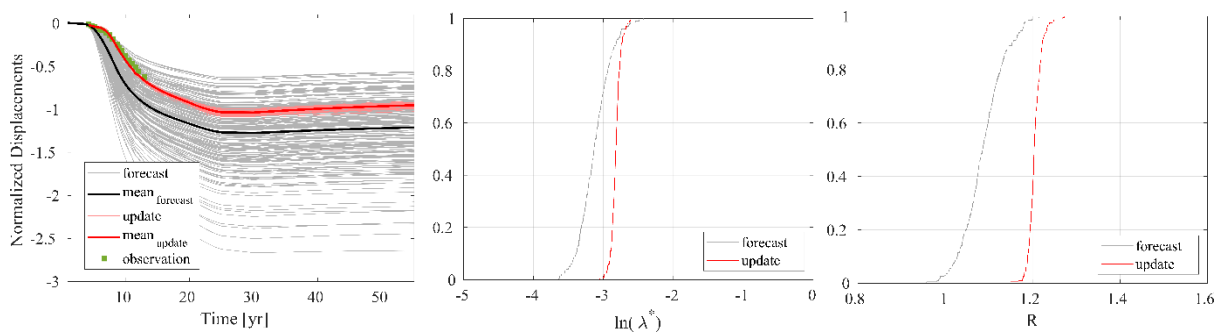


Figure 5 ES application for the VEP model at year 13.

Conclusion

A comprehensive workflow based on a sequential data-integration approach has been developed and applied to a real-world off-shore reservoir in Italy. The land subsidence model is progressively trained in time through the assimilation of new data, with an increasing reduction of the uncertainties. Even though at some points non-univocal parameter updates can be encountered, displacement ensembles are effectively and progressively constrained, providing more and more reliable predictions that can be of great help in supporting decision-making processes. Future developments concern the use of the proposed approach to identify the most influential class of measurements to better improve the model prediction, so as to drive the effective design of the most useful monitoring programs.

References

- P. A. Fokker, B. B. T. Wassing, F. J. van Leijen, R. F. Hanssen, D. A. Nieuwland, Application of an ensemble smoother with multiple data assimilation to the Bergermeer gas field, using PS-InSAR. *Geomechanics for Energy and the Environment* 5 (2016) 16–28. doi:10.1016/j.gete.2015.11.003.
- L. Gazzola, M. Ferronato, M. Frigo, C. Janna, P. Teatini, C. Zoccarato, M. Antonelli, A. Corradi, M. C. Dacome, S. Mantica. A novel methodological approach for land subsidence prediction through data assimilation techniques. *Computational Geosciences* 25 (5) (2021) 1731–1750. doi:10.1007/s10596-021-10062-1.

G. Isotton, P. Teatini, M. Ferronato, C. Janna, N. Spiezia, S. Mantica, G. Volonté. Robust numerical implementation of a 3D rate-dependent model for reservoir geomechanical simulations. *International Journal for Numerical and Analytical Methods in Geomechanics* 43 (18) (2019) 2752 – 2771. doi: 10.1002/nag.3000

M. Nepveu, I. C. Kroon, P. A. Fokker, Hoisting a Red Flag: An Early Warning System for Exceeding Subsidence Limits. *Mathematical Geosciences* 42 (2010) 187–198. doi:10.1007/s11004-009-9252-2.

P. J. Van Leeuwen, G. Evensen, Data assimilation and inverse methods in terms of a probabilistic formulation., *Monthly Weather Review* 124 (12) (1996) 2898–2913. doi:10.1175/1520-6720(1996)124<2898:DAAIMI>2.0.CO;2